

Direct Local Electric Field Measurements in the Sheaths of the ICRF Antenna in IShTAR

Ana Kostic^{1,2,3,a)}, Kristel Crombé^{1,4}, Ralph Dux², Michael Griener², Mari Usoltceva^{1,2,5}, Ilya Shesterikov², Elijah H. Martin⁶ and Jean-Marie Noterdaeme^{1,2}

¹*Ghent University, Department of Applied Physics, Ghent, Belgium.*

²*Max Planck Institute for Plasma Physics, Garhing, Germany.*

³*Ludwig Maximilian University of Munich, Munich, Germany.*

⁴*LPP-ERM-KMS, TEC partner, Brussels, Belgium.*

⁵*Université de Lorraine, Nancy, France.*

⁶*Oak Ridge National Laboratory, Oak Ridge, Tennessee, USA.*

^{a)}Corresponding author: Ana.Kostic@ipp.mpg.de

Abstract. An important step in understanding the Radio Frequency sheaths in the vicinity of Ion Cyclotron antennas in magnetically confined fusion plasmas is to benchmark the existing theoretical models against real antenna operation. The data needed is the local DC electric field that develops in the sheaths surrounding the plasma-facing structures of the antenna. In this contribution we present our most recent progress on the development of a spectroscopic diagnostic, which delivers direct and local measurements of the electric field across the sheath. The method uses polarization spectroscopy where the electric fields are optically determined from the Stark shift of the emission spectra of excited helium atoms. The sheath electric fields obtained with this diagnostic scheme are measured in the vicinity of the ICRF antenna in IShTAR, a test facility designed to mimic the tokamak edge plasma parameters and focused on studying the ICRF antenna-plasma interaction.

INTRODUCTION

Despite the reliable application of waves in the Ion Cyclotron Range of Frequencies (ICRF) for heating and current-drive in magnetically confined toroidal fusion plasmas, unfavourable side-effects of their operation in such devices remain. The wave launchers, ICRF antennas, must be placed close to the plasma edge to ensure the plasma densities needed to propagate the dominant mode, the Fast Wave. This, in return, establishes interactions between the antenna's front faces and the plasma edge, which are amplified by the strong RF near fields.

Indirect studies of ICRF antenna-edge plasma interactions suggest [1, 2, and references therein] that the root of the problem is the rectification of the RF fields in the sheath surrounding the antenna's plasma facing components. This introduces strong DC electric fields across the sheaths, which accelerate plasma ions, thereby enhancing sputtering and release of impurities to the main plasma.

Since the intensified impurity release from the antenna's plasma-facing structures was first observed, the design of ICRF antennas and their operation schemes have improved to minimise these side-effects [3]. The contemporary focus of the ICRF community is on computational codes designed to study, model and predict the antenna-plasma edge interaction, which is of critical importance to the ICRF systems used in the next step fusion devices and long-pulse burning plasmas. These computational codes have grown and improved on an ongoing basis [4]. Yet, to validate their predictions against actual antenna operation, the key ingredient missing is the electric field measured directly in the sheaths.

Non-invasive measurements of electric fields in plasma are typically achieved spectroscopically. The electric field strength can be determined directly from the Stark effect on the spectral lines of emitting plasma species [5, 6, 7]. This has also been applied in our work, motivated by earlier validation of the observable Stark effect in the plasmas of interest - namely in front of the Lower Hybrid Antenna in tokamaks and for the studies of the ICRF waves on capacitively coupled discharges [5, 6, 8].

Stark effect on helium triplet 447 nm line - diagnostic method

Under the influence of a strong external electric field, the electronic configuration of emissive atomic species will change. This can be observed as a modification of the emission spectrum - as a result of the splitting and mixing of the energy levels of an atom (or ion) in an external electric field, the wavelength of a spectral line corresponding to a certain transition between two of these levels will shift from its unperturbed value, and additional spectral lines may appear. In addition to energy levels being redistributed, each level consists of sub-levels with different magnetic quantum number. The transitions between different sub-levels will give emission of distinct polarization (e.g, polarization parallel to the electric field vector, i.e. π , or perpendicular to it - σ), the wavelength of which is also in this case dependent on the macroscopic electric field. The quantification of these changes in the emission spectrum is therefore a direct evaluation of the strength of the electric field to which atomic species were exposed.

Our diagnostic method is based on the Stark effect on transitions of neutral helium. The main reason behind this choice is the availability of the gas in the test stand used for the experiments (see the following Section). The advantage of choosing helium also lies in the fact that the Stark effect is more prominent for lighter than for the heavier elements, such as argon, which increases the diagnostic sensitivity.

The choice of the particular transition, a 4D-2P triplet, or a corresponding 447 nm spectral line, is simply due to the fact that this particular line was observed with the best signal-to-noise ratio in our experiments. As the prime quantum number, n , increases, so does the sensitivity of a transition to an external electric field, while the emission intensity decreases. Hence, for the environment in which our experiments were conducted, this atomic transition was a balance between the two.

The effect of increasing electric field strength on the spectral line, and the additional “forbidden” component is shown in Fig. 1. These synthetic spectra are created with the EZSSS - Explicit Zeeman Stark Spectral Simulator code [6]. The code first recalculates the energy levels by solving Schrödinger equation for each electric field strength, and specified experimental geometry (magnetic and electric field vector orientation, view line and the polarization plane, which in the case for the Fig. 1 was perpendicular). This finds the discrete spectral lines corresponding to the chosen transition. As the final output EZSSS provides continuous spectra created by convoluting the discrete spectral lines with broadening mechanisms, taking into account instrumental and Doppler broadening of the experimental set-up.

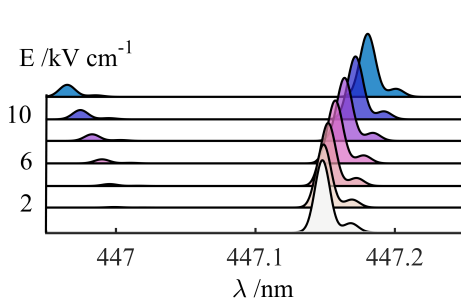


FIGURE 1. Synthetic spectra demonstrate a wavelength shift of 447 nm line of He due to Stark effect with increasing intensity of macroscopic electric field

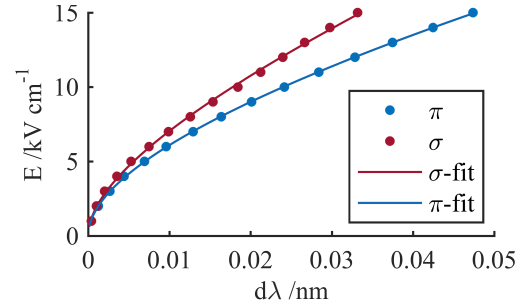


FIGURE 2. Wavelength shift of the main component with increasing intensity of electric field, compared for the parallel, π , and perpendicular, σ , polarization

The wavelength shift of the main (strongest) 447.147 nm line, $d\lambda$, as a function of the electric field strength for the geometry applied in our experiments, is shown in Fig. 2. From this figure it becomes clear that the polarizing filter should be included in the experimental optical arrangement to allow only the more sensitive π -polarized emission for the diagnostic purposes. The line of the best fit through the points of the shifts with π polarization is described with:

$$E[\lambda_0 = 447.147 \text{ nm} | \text{kV cm}^{-1}] = 65.91 \times d\lambda[\text{nm}] + 54.35 \times d\lambda[\text{nm}]^{0.5}, \quad (1)$$

which will be used to evaluate the electric fields from experimentally observed Stark shifts.

DIAGNOSTIC IMPLEMENTATION IN IShTAR

The spectroscopic diagnostic was set-up and tested in IShTAR, for measuring the electric field in the sheath of its ICRF antenna. The machine was described in Ref. [9, 10] in detail. In this section we will introduce the diagnostic

implementation in this device, as an improvement in terms of precision and correctness from the already tested setup [8]. The spectra analysis remains the same as in [8], with changes being applied only to the geometry which is captured within Eq. 1.

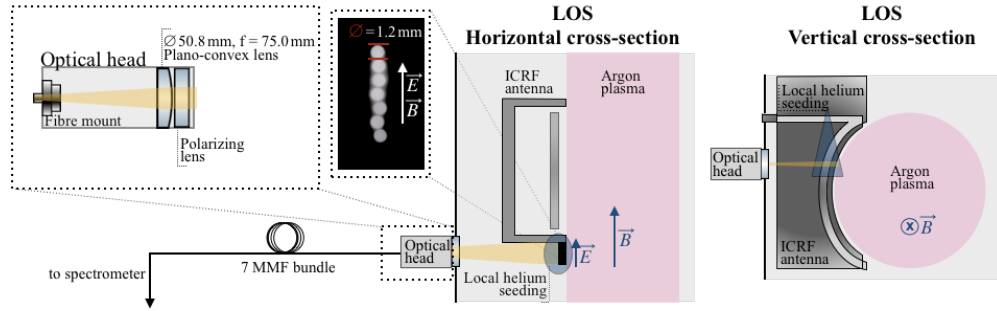


FIGURE 3. Schematic view of the electric field diagnostic implemented in IShTAR

In the main vacuum chamber, IShTAR has a dedicated single-strap ICRF antenna, operating at 5.9 MHz frequency, matched by a variable capacitor and inductor prior to a plasma discharge. The antenna is carefully designed to follow the shape of the plasma column created in the helicon source and is fixed inside a stainless-steel case. Two sets of coils are wound around the main vacuum chamber, in Helmholtz-like configuration, providing magnetic field along the machine's main axis. The magnetic field established during the demonstrative discharges described in the following section, at the location of the electric field measurements was $B \approx 90$ mT, a value too low for the Zeeman effect to introduce any detectable change on the spectral line shape and wavelength.

Our interest is in the sheaths that develop around the antenna's casing, where the background magnetic field and rectified DC electric field will be parallel to each-other. To measure this electric field, the optical head is installed on the port behind the ICRF antenna, providing a view-line along its side (Fig. 3). The optical head contains a polarizing filter and an $f = 75$ mm lens that couples the light from the area of interest to the bundle of fibres. The bundle itself contains seven $\varnothing 200 \mu\text{m}$ multi-mode (MMF) fibres arranged at both ends in a linear configuration.

The other end of the bundle is connected to the entrance slit of the Andor Shamrock 750 spectrometer. This spectrometer is in Czerny-Turner optical arrangement, with a focal length of 750 mm, providing high optical resolution, particularly since the grating used in this study is of 3600 lines per mm. The resolved spectra are finally detected and recorded with the Andor's iStar 334 CCD detector. The instrumental function of the configuration is 0.01 nm, or about 6 pixels. High spectral resolution at the expense of the optical (spatial) one is a feature of Czerny-Turner optical arrangement with large focal length. That is why the seven fibres in a bundle provide only one spectrum per acquisition from the area of interest with dimensions $1.2 \text{ mm} \times 8.4 \text{ mm}$.

IShTAR can operate with either argon or helium plasma. However, with argon it achieves better plasma performance. We operate in argon plasma with the local helium gas seeding to achieve a localized measurement of the electric field in the antenna's vicinity. The seeding is supplied with a gas tube installed above the area of interest. Careful calibration of the flow rate of both gasses was done to maintain good plasma properties, but also to provide sufficient signal for the electric field diagnostic. With the continuous flow of helium, the amount of injected atoms in each second is 2.7×10^{19} .

DEMONSTRATIVE RESULTS AND DISCUSSION

The single most striking observation to emerge while creating a database of discharges that used this diagnostic was that the shifts of the spectral lines do not seem to distinguish whether the power was delivered to an ICRF antenna or not (the cases referred to as "ICRF being on" and "off"). An example of this can be seen in Fig. 4. There is an evident wavelength shift of the experimental lines from the unperturbed spectral line profile recorded from the calibration lamp. According to Eq. 1 this wavelength shift of the spectrum recorded during the discharge in which ICRF was on, $d\lambda = 0.002 \text{ nm}$, corresponds to an electric field of $E = 2.56 \text{ kV cm}^{-1}$. However, there is virtually no relative shift between the two lines recorded from the area of interest during the discharges which differ only in that the ICRF was on or off. In both cases the electric field has the same value, within the error-bar. The Stark shift of

the spectral line recorded during the discharge without an ICRF is $d\lambda = 0.0015$ nm, corresponding to electric field of $E = 2.22$ kV cm⁻¹.

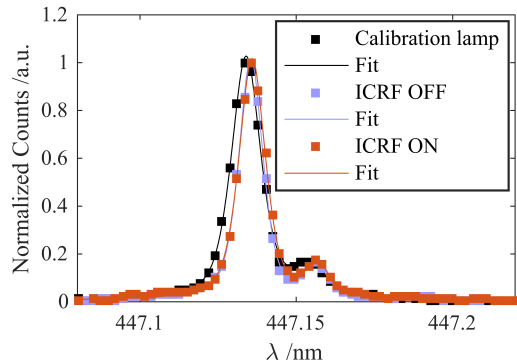


FIGURE 4. Fitted spectral lines of helium calibration lamp and the two experimental results demonstrate a wavelength shift due to macroscopic electric field in the sheath of an ICRF antenna.

One reason why this could occur is that the power on IShTAR’s antenna is simply too low for the RF sheath effects to surpass the voltage drop in classical thermal sheath. The maximum power supplied from the generator is 1 kW, which was also the value used for all of the compared discharges. The other hypothesis is that the location of the measurements, near the casing of the ICRF antenna, is poloidally inbetween the upper and lower corner of the casing, where the rectified rf sheath effects are weaker. Finally, as implied by the simulation of IShTAR’s ICRF waves and plasma conditions (background magnetic field strength and the radial electron density profile in front of IShTAR’s antenna), developed in [11], during these discharges the plasma densities near the antenna ($n_e = 2 - 2.5 \times 10^{16}$ m³) were two orders of magnitude too high to allow the Slow Wave propagation cone to leave the ICRF antenna casing[12].

CONCLUSIONS

A spectroscopic diagnostic is implemented in IShTAR to measure electric fields in the sheaths of its ICRF antenna. The diagnostic method was explained in this contribution together with illustrative results - an example spectra from two discharge configurations differing only in that the ICRF antenna was used in one and not in the other. Within these results, there is no significant difference between the two cases, in terms of the electric fields established across the sheath of an ICRF antenna.

The next step of the diagnostic development is to install additional optics that will help isolate the optical signal from each fibre in a bundle on the end connected to the spectrometer, allowing for the spatially resolved measurements. The observation made with this diagnostic highlights an important issue requiring further investigation and potential optimization of IShTAR’s discharges towards the experimental study of the RF sheaths. Nevertheless, these results are seen as a successful test for non-helium plasma diagnostic operation, with local gas seeding, and the new optical arrangement with the fibre bundle.

ACKNOWLEDGMENTS

This work has been carried out within the framework of the EUROfusion Consortium and has received funding from the Euratom research and training programme 2014-2018 and 2019-2020 under grant agreement No 633053. The views and opinions expressed herein do not necessarily reflect those of the European Commission.

REFERENCES

- [1] D. A. D’Ippolito, J. R. Myra, M. Bures, and J. Jacquinet, *Plasma Physics and Controlled Fusion* **33**, 607–642 (1991).
- [2] J.-M. Noterdaeme and G. Van Oost, *Plasma Physics and Controlled Fusion* **35**, 1481–1511 (1993).
- [3] V. Bobkov *et al.*, *Plasma Physics and Controlled Fusion* **59**, p. 014022 (2017).
- [4] L. Colas *et al.*, *EPJ Web of Conferences* **157**, p. 01001 (2017).
- [5] C. C. Klepper *et al.*, *Physical Review Letters* **110**, p. 215005 (2013).
- [6] E. H. Martin, “Electric field measurements of the capacitively coupled magnetized RF sheath utilizing passive optical emission spectroscopy,” Ph.D. thesis, North Carolina State University, Raleigh 2014.
- [7] N. Cvetanović, M. M. Martinović, B. M. Obradović, and M. M. Kuraica, *Journal of Physics D: Applied Physics* **48**, p. 205201 (2015).
- [8] A. Kostic, R. Dux, K. Crombé, A. Nikiforov, R. Ochoukov, I. Shesterikov, E. H. Martin, and J.-M. Noterdaeme, *Review of Scientific Instruments* **89**, p. 10D115 (2018).
- [9] K. Crombé *et al.*, in *Plasma science and technology : basic fundamentals and modern applications* (IntechOpen, 2019).
- [10] I. Shesterikov *et al.*, *Review of Scientific Instruments* **90**, p. 083506aug (2019).
- [11] M. Usoltceva, “Advancements in langmuir probe diagnostic for measurements in rf sheath and in modelling of the icrf slow wave,” Ph.D. thesis, Ghent University 2019.
- [12] M. Usoltceva *et al.*, *Plasma Physics and Controlled Fusion* (Manuscript accepted for publication).